

LINE 1970-20

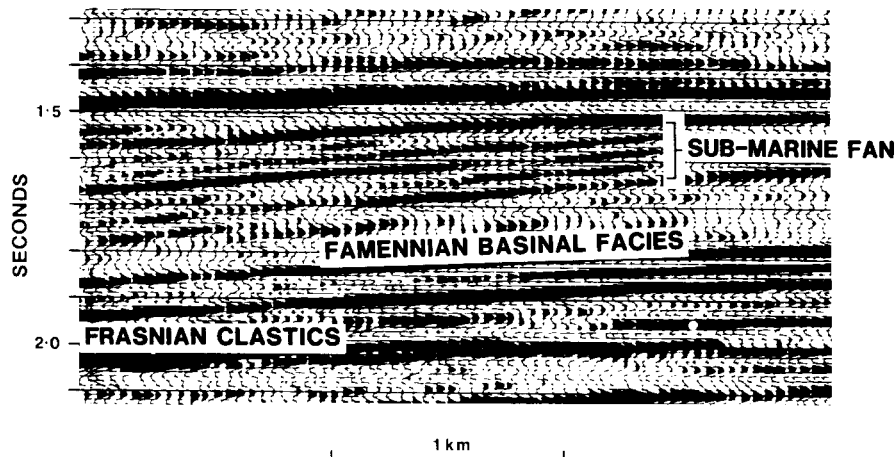


FIGURE 6
Seismic line 1979-20 (right hand side is SE) near site B, showing a possible sub-marine fan.

expression of this regression is strongly developed near site B (Fig. 1). A NW-SE trending seismic section through site B shows the toplap truncations between 1.5 and 1.6 seconds (Fig. 6). This sequence is interpreted as a sub-marine fan developed on the shelf slope of the Lennard Shelf. The sub-marine fan may be a distal clastic expression of the well documented fan deltas feeding the Lennard Shelf from the Kimberley Block.

Conclusions

The present study has developed a relative sea-level curve, based on seismic sequence analysis, for the northern Canning Basin. Hydrocarbons appear to be trapped preferentially in sequences deposited during relative sea-level low stands. The Nullara Cycle reefs, deposited during the late Devonian low stand, have a characteristic trough-on-peak wavelet response. Clastic sub-marine fans may have developed during the initial low stand in the early Carboniferous (Yellow Drum Formation deposition); oil in the Blina field is trapped in carbonates deposited during this low stand.

A number of disparate threads have been drawn together through the present analysis of sea-level changes in the northern Canning Basin. The preference for hydrocarbons to be trapped in units deposited during sea-level low stands, while possibly an obvious association in retrospect, is a valuable observation re-affirmed by this study.

References

- Brown, J. F., Jr. & Fisher, W. L. (1977)—'Seismic-stratigraphic interpretation of depositional systems: examples from Brazilian rift and pull-apart basins, in Payton, C. E. (Ed.), *Seismic stratigraphy—applications to hydrocarbon exploration*: AAPG *Memoir* 26, 213-248.
- Brown, J. F., Jr. & Fisher, W. L. (1979)—'Seismic stratigraphic interpretation and petroleum exploration': Continuing Education Course Note Series, No. 16, AAPG, Tulsa, Ok., 56p.
- Harland, W. B., Cox, A. V., Llewellyn, P. G., Pinkton, C. A. G., Smith, A. G. & Walters, R. (1982)—'A geologic time scale': Cambridge University Press, 131p.

- Mitchum, R. M., Jr. & Vail, P. R. (1977)—'Seismic stratigraphy and global changes of sea level, part 7': seismic stratigraphic interpretation procedure, in Payton, C. E. (Ed.), *Seismic stratigraphy—applications to hydrocarbon exploration*: AAPG *Memoir* 26, 135-143.
- Moors, H. T., Gardner, W. E. & Davis, J. (1984)—'Geology of the Blina oilfield, in Purcell, P. G. (Ed.), *The Canning Basin, W.A.*: Proceedings of Geol. Soc. Aust./Pet. Expl. Soc. Aust. Symposium, Perth, 1984, 277-283.
- Norris, D., Taylor, D. & Hall, J. (1984)—'Some results of high resolution seismic surveying in the Sundown area, northern Canning Basin, W.A., in Purcell, P. G. (Ed.), *The Canning Basin, W.A.*: Proceedings of Geol. Soc. Aust./Pet. Expl. Soc. Aust. Symposium, Perth, 1984, 319-327.
- Playford, P. E. (1980)—'Devonian Great Barrier Reef of the Canning Basin, Western Australia': AAPG Bull., v. 64, 814-840.
- Playford, P. E. (1984)—'Platform-margin and marginal-slope relationships in Devonian reef complexes of the Canning Basin, in Purcell, P. G. (Ed.), *The Canning Basin, W.A.*: Proceedings of Geol. Soc. Aust./Pet. Expl. Soc. Aust. Symposium, Perth, 1984, 189-214.
- Rasidi, J. S. (1978)—'Buried reef structures in the Lennard Shelf, Canning Basin, Western Australia': BMR Journal of Australian Geology & Geophysics, v. 3, 80-83.
- Vail, P. R., Mitchum, R. M., Jr. & Thompson, S., III, (1977)—'Seismic stratigraphy and global changes of sea level, part 4: global cycles of relative changes of sea level, in Payton, C. E. (Ed.), *Seismic stratigraphy—applications to hydrocarbon exploration*: AAPG *Memoir* 26, 83-97.

DEPHASING OF SEISMIC SECTIONS

N. J. Moriarty and S. A. Greenhalgh

Introduction

A perennial problem in the processing and interpretation of seismic data from the Cooper-Eromanga Basin is the estimation and subsequent removal of the wavelet phase. There are many non-geological factors such as vibrator coupling, geophone characteristics, anelastic absorption,

instrument response and processing sequence which affect the wavelet phase.

The conversion of seismic data to zero phase is generally considered desirable so as to maximise resolution, and is critical for any stratigraphic delineation or if attribute processing is being contemplated. Within some oil companies, it is common practice to apply arbitrary constant phase shifts to the seismic section, usually in multiples of 90° , in an attempt to return the traces to 'normal' polarity, and thus facilitate comparisons of seismic data of different vintage or shot by different crews. However the wavelet, and hence the seismic trace, is unlikely to be constant phase (much less zero phase), even for Vibroseis data. The constant phase subtraction process can therefore produce spurious features on the seismic section.

Uncertainty concerning the phase of a seismic section can always occur when well synthetic traces of various phase can be bulk time shifted to yield several similar matches with the actual seismic trace. The problem is to disentangle wavelet phase from the constant time shifts associated with statics and anti-alias filter delays.

A usual assumption in the statistical determination of a wavelet from seismic data is that the reflectivity series has a white amplitude spectrum. Most well log reflection coefficient series studied by us are not white (consistent with the findings of Walden and Hosken (1985)), and in particular, lack the lower frequencies which dominate the Vibroseis sweep range (10–70 Hz).

Wavelet Phase Extraction by Cross Correlation

An alternative approach to extracting the phase spectrum (only) of the wavelet is by cross correlating the seismic data with the drift corrected well reflectivity series. Synthetic examples using a variety of band limited constant phase wavelets show that the method can recover phase from low noise data with an accuracy of a few degrees. Figure 1 illustrates the application of the cross correlation method with a test case, zero-phase wavelet (200 ms length, 10–55 Hz) and the real reflectivity series at Merrimelia 18 well, used to produce the synthetic trace. Diagram (d) shows the time domain cross-correlation of this synthetic trace with the drift corrected reflectivity series, after the synthetic trace has been delayed by 10 ms. Diagram (e) shows the equivalent result in the frequency domain. The resulting phase spectrum yields an intercept of 0° (zero-phase wavelet) and a slope of -10 ms. It is readily apparent that the wavelet as well as the bulk time shift have been accurately recovered.

Structural Deconvolution

The complete wavelet, specified in terms of both the amplitude and phase spectrum, can be recovered at the well by structural deconvolution of the seismic trace with the drift-corrected well reflectivity series (see Danielsen and Karlsson (1984)). Exact inverse filtering by Fourier division and Wiener time domain optimum filtering have been performed on a wide range of synthetic examples to study the effect of noise,

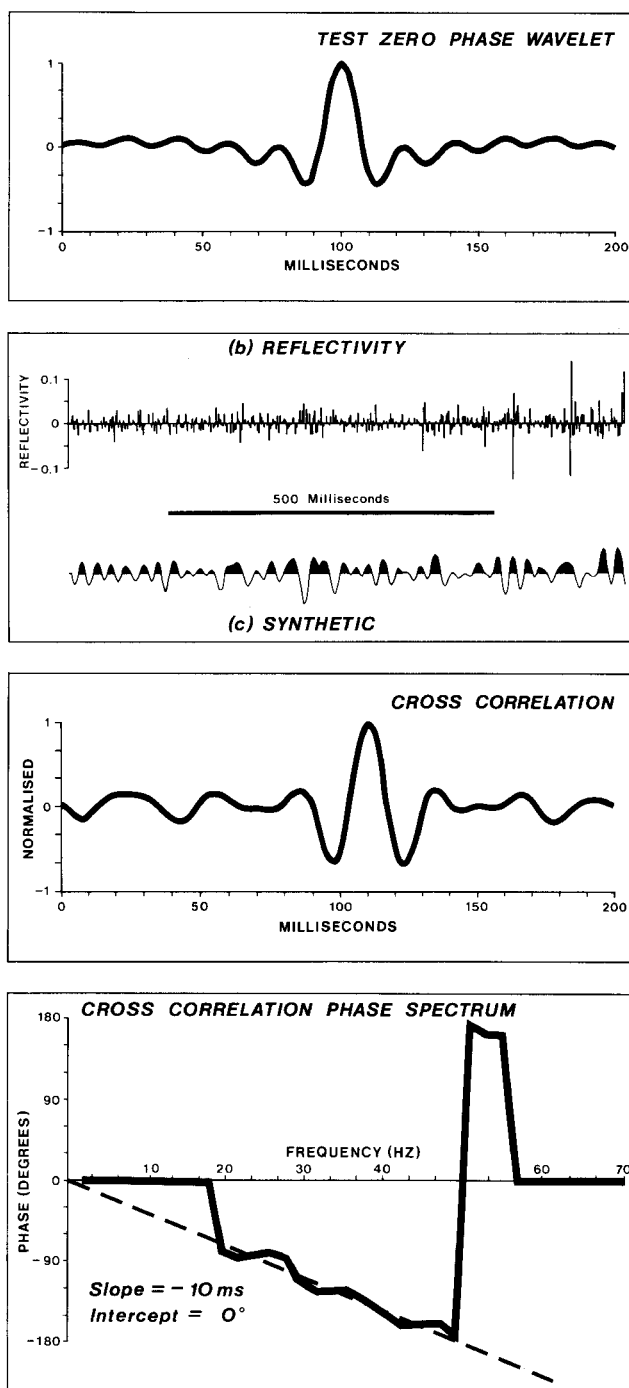


FIGURE 1
 Synthetic examples showing application of cross-correlation method of wavelet recovery. The synthetic trace (Diagram (c)) is obtained by convolving the zero-phase wavelet (a) with the reflectivity series (b). The synthetic has been bulk shifted by 10 ms. Cross correlation of synthetic with the reflectivity yields the trace of Diagram (d). The phase spectrum of the cross correlation is shown in Diagram (e). Although the amplitude spectrum of the actual wavelet cannot be removed, the phase is correct, yielding zero phase and a 10 ms pulse delay.

wavelet phase, time-varying misties in the well-log, bulk time shift in the seismic data, and length of data window used. Both these two techniques, as well as cross correlation, require the application of a taper window to the reflectivity and synthetic trace to prevent reflectivity outside the data

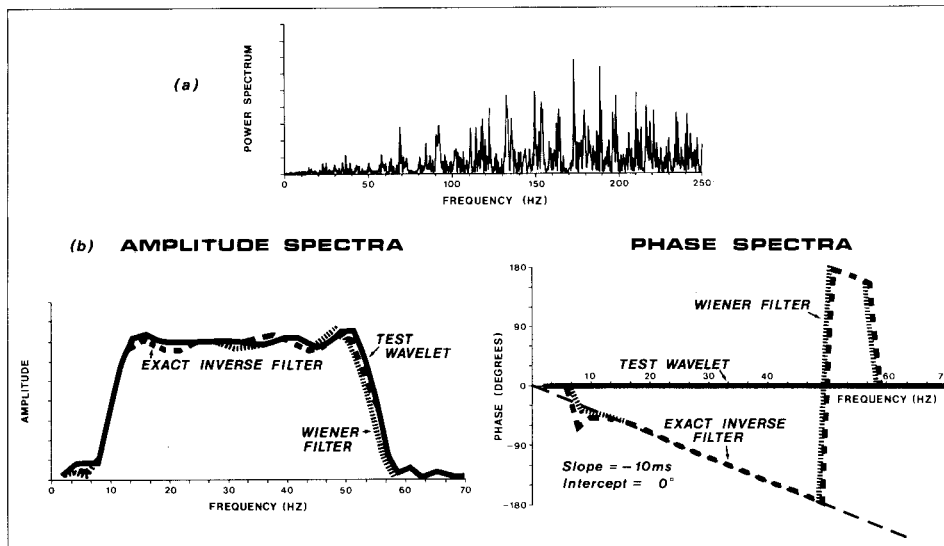


FIGURE 2

Application of exact inverse filtering and Wiener filtering to the synthetic data of Figure 1. Diagram (a) depicts the clearly non-white power spectrum of the reflectivity series (see Figure 1b) at Merrimelia 18. The recovered amplitude and phase spectra of the exact inverse and Wiener wavelets (Diagram (b)) agree with the actual pulse, apart from the bulk time shift of 10 ms which appears as the linear term in the recovered phase spectra.

window contributing to the wavelet convolution. A half cosine bell applied to the beginning and end of the data over a window of half the anticipated length of the wavelet is adequate.

Figure 2 shows the results of wavelet spectrum recovery from the synthetic trace and reflectivity series of Figure 1, for both the exact inverse and Wiener filters. Note the non-whiteness of the reflectivity spectrum at Merrimelia 18. Upon inverse

Fourier transformation of the data for the exact inverse filter and Wiener filter, the time domain wavelets of Figure 3 are obtained. Note the close agreement in pulse shape with the actual (synthetic) wavelet, and the time delay (deliberately introduced) of 10 ms. The filter performance parameter (P), which is a measure of the difference between actual and desired output, indicates that phase and bulk time shift can be determined satisfactorily from data contaminated by even a high level of white noise. This parameter, identified in brackets to the right of Figure 3, suggests a comparable performance for the exact inverse and Wiener filters. In the presence of medium to high noise, the Wiener filter yields a slight improvement. The seismic wavelet, once determined, can then be used to deconvolve reflection records shot away from the well.

A Field Example

The exact inverse and Wiener filters have been successfully applied to deconvolve real seismic data at the Merrimelia 18 well, Cooper Basin. Figure 4(a) shows the phase spectrum of the exact inverse filter wavelet. It is apparent that a bulk time delay of 20 ms exists between the seismic trace and the well reflectivity series. This bulk time shift (static) is then removed by advancing the seismic trace by 20 ms. Figure 4(b) shows the time-domain result of the wavelet recovery using all three techniques — cross correlation, exact inverse filtering and Wiener filtering. The filter performance parameter takes on normalised values of 0.88 and 0.91 for the latter two approaches, respectively. Figure 5 shows the frequency domain spectra of these wavelets. The recovered wavelet, although non-linear, has an average phase of -60° and bulk time shift relative to the well synthetic of 20 ms. Figure 6 shows the original seismic trace at the Merrimelia 18 well and the same trace with linear phase shifts of 60° , 90° , 180° and -90° . In addition the fully deconvolved (zero phase) trace produced using the exact wavelet is also shown. It is clear from this

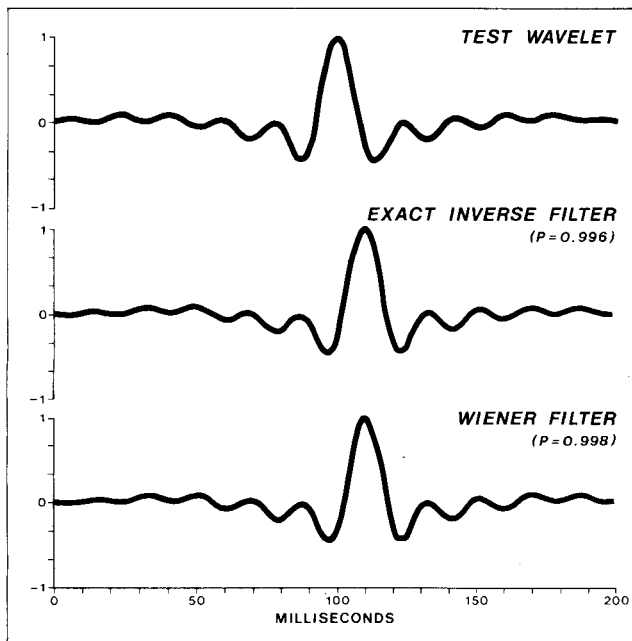


FIGURE 3

Time-domain results of wavelet recovery obtained by inverse Fourier transformation of the exact inverse and Wiener filters data of Figure 2. The filter performance parameter P, which is close to 1, implies an excellent result.

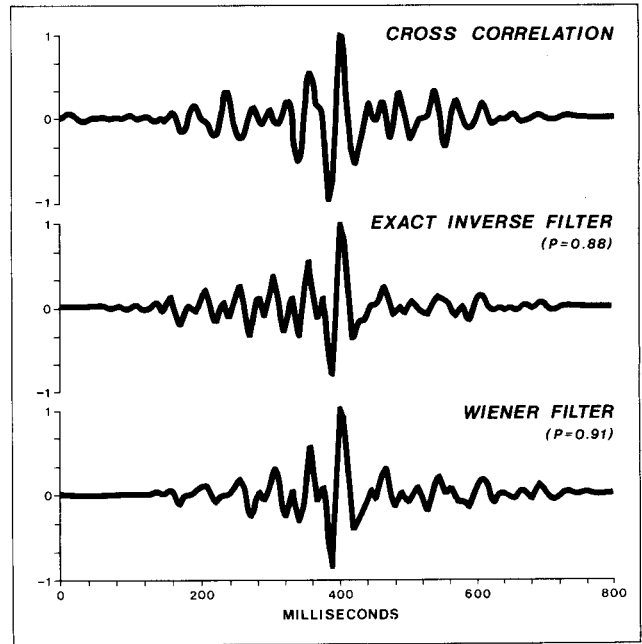
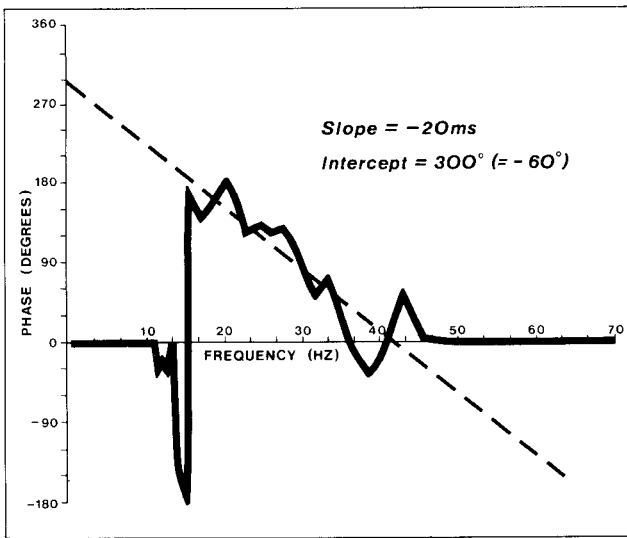


FIGURE 4

- (a) Phase spectrum for exact inverse filter recovery of the wavelet at Merrimelia 18. The actual seismic trace has been deconvolved using the well reflectivity series. The wavelet has an average phase of -60° and a bulk time shift of -20 ms.
- (b) Time-domain results of wavelet recovery at Merrimelia 18, using techniques of cross-correlation, exact inverse filter, and Wiener filter. The Wiener filter ($P = 0.91$) yields the best result.

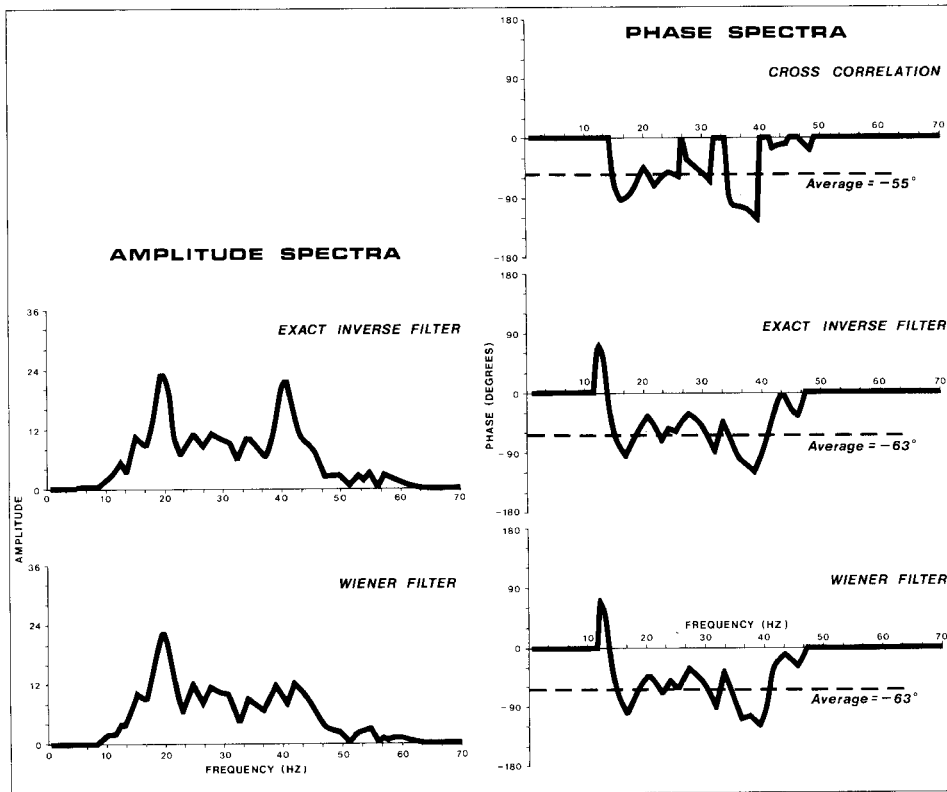


FIGURE 5

Amplitude and phase spectra of the recovered wavelet at Merrimelia 18, using all three techniques after time shifting the seismic trace to remove the 20 ms delay (see Figure 4).

example that blind application of $\pm 90^\circ$ or 180° phase shifts to the seismic data can produce serious discrepancies with the well synthetic, and results in a record that is inferior to the fully deconvolved trace.

Further tests at other well locations are now in progress to establish the constancy of the extracted wavelet and the stability of this approach.

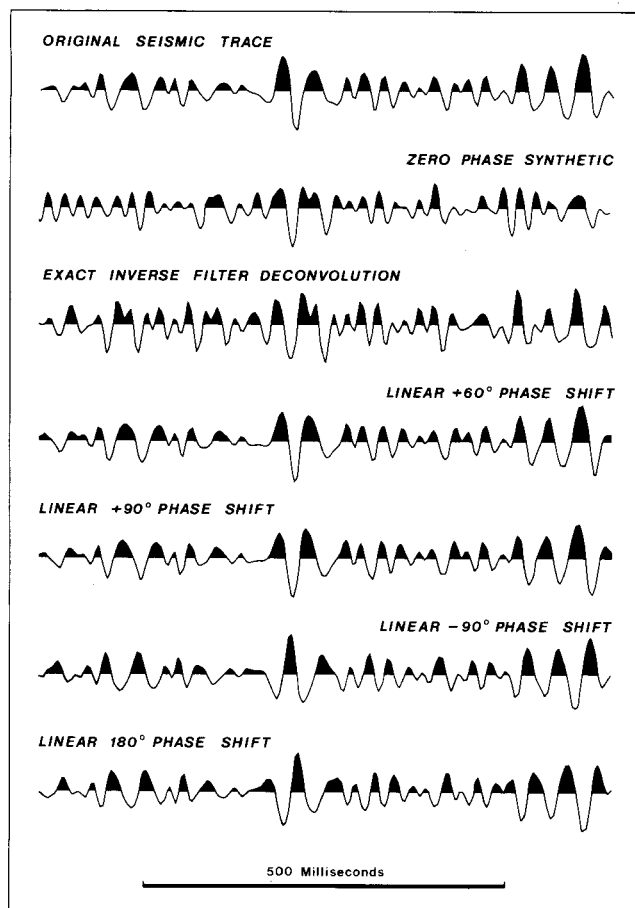


FIGURE 6
Structural deconvolution of seismic data at Merrimelia 18. Note the close agreement between the zero-phase synthetic and the result of exact inverse filtering. The results of constant phase shifting ($+60^\circ$, $+90^\circ$, -90° , 180°) of the original seismic trace are shown alongside for comparison. Note the difficulty of estimating phase visually, and the inferior result that a phase shift produces.

References

- Danielsen, V. & Karlsson—T. V. Extraction of signatures from seismic and well data. *First Break*. 2/4, 15–21.
 Walden, A. T. & Hosken, J. W. J. (1985)—An investigation of the spectral properties of primary reflection coefficients. *Geophys. Pros* 33, 400–435.

THE GEOPHYSICAL DISCOVERY OF THE ABRA BASE METAL DEPOSIT, BANGEMALL BASIN, WESTERN AUSTRALIA

A. J. Mutton and P. M. McInerney

Introduction

The Abra base metal deposit is located about 900 km NNE of Perth, W.A. (Fig. 1) at the eastern end of the Jilawarra

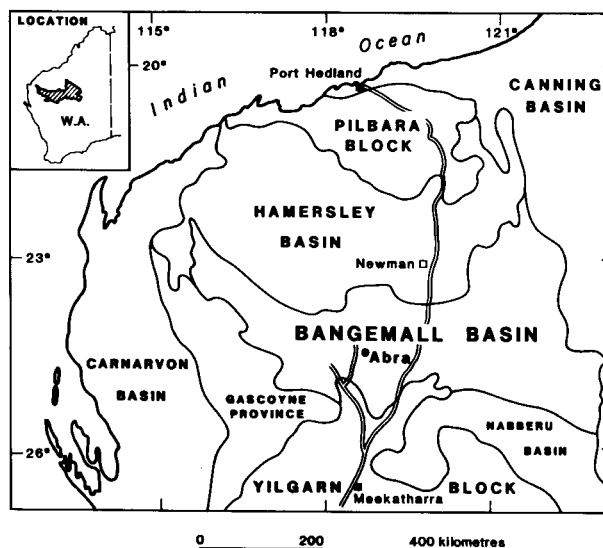


FIGURE 1
Location of Abra base metal deposit, Bangemall Basin, W.A.

Mineralized Belt, a structurally controlled zone of mineralized clastic and carbonate sediments forming the oldest rock units of the Middle Proterozoic Bangemall Basin (Muhling & Brakel, 1984). The deposit was discovered following the delineation and interpretation of a coincident source of magnetic and gravity anomalies. Subsequent drilling of this source had outlined a large tonnage, low grade polymetallic mineralized body, regarded as a significant new style of mineralization for its environment (Boddington, 1986).

In this paper, we present the geophysical evidence and interpretation which led to the discovery of Abra. We also present the results of other geophysical methods over the deposit, which is considered to be totally 'blind' to routine surface geological and geochemical exploration techniques.

Geological Setting and Initial Exploration

The rocks of the Jilawarra Belt were deposited in an interpreted graben structure, produced by rifting of the Yilgarn and Pilbara cratons. Associated with this rifting appear to be several centres of mineralization, which have been structurally controlled and in places deformed by subsequent folding and faulting. Details of the stratigraphic and structural relationships are contained in Muhling & Brakel (1984).

The Jilawarra Belt was first recognised as a significant mineralized province after the discovery by Amoco Minerals Australia Company in 1974 of a shallow base metal deposit, and subsequently several other mineralized occurrences along a 50 km strike length. Airborne magnetic surveys were carried out over the belt to aid geological mapping and to identify possible base metal targets.

The Abra prospect was identified in 1976, when an airborne magnetic survey using 400 m line separation delineated a distinctive 400 nT isolated magnetic anomaly. Figure 2 shows the magnetic contour map of the prospect derived from a later more detailed airborne survey (200 m line spacing).